

Methods

Plasmids

Hoxa9, *Trib1* and *Erg* cDNAs were cloned into pMYs retroviral vectors. Lentivirus plasmids containing short hairpin RNA (shRNA) constructs of mouse *Erg*, *Cebpa*, human *TRIB1* and non-target control were purchased from Sigma (Sigma-Aldrich). A lentivirus plasmid containing short guided RNA (sgRNA) for *Erg* was purchased from Addgene. The shRNA and sgRNA sequences are listed in supplemental Table 1.

Cell lines and cell culture

Bone marrow cells were prepared from an eight-week-old female *Trib1*^{ko/ko} mouse five days after injection of 150 mg 5-fluorouracil/kg body weight (Kyowa Hakko Kirin). Bone marrow cells were cultured for 24 h in IMDM (Invitrogen) supplemented with 10% fetal bovine serum (FBS; HyClone), ten ng/mL IL-6, ten ng/mL IL-3 and 100 ng/mL SCF (R & D Systems). Retroviral stocks of pMYs-*Hoxa9*-IRES-mKO and pMYs-FLAG-*Trib1*-IRES-EGFP were added to the medium containing bone marrow cells with six μ g/mL Polybrene (Sigma) and then spun at 1400 g for two hours. Expression of *Hoxa9* and *Trib1* was confirmed by detecting kusabira orange (mKO) and EGFP by flow cytometry as well as immunoblotting. *Trib1* hi and null cells were maintained in IMDM medium containing 10% FBS and ten ng/mL IL-3. Human HEL, KU812, P39, HL-60 and THP1 AML cells were maintained in RPMI-1640 supplemented with 10% FBS

Mice and bone marrow transplantation

Trib1 conditional knock-out mice were generated by inserting loxP sequences in *Trib1* intron 1 and at 325 bp downstream of exon 3. The mice were mated with ROSA26-Cre deleter mice and a germline knockout allele was created. All mice are on C57Bl/6 background. C57Bl/6J recipient mice were irradiated (4 Gy for assays with cell lines; MBR-1520A. Hitachi Medico) and injected with leukemic cells. Leukemic cells were injected via tail vein. Mice were monitored daily for evidence of disease, and smears of peripheral blood were examined every week. The onset of AML was determined by detecting when immature myeloid cells constituted at least 20% of the leukocytes in peripheral blood. All of the diseased mice were subjected to autopsy and analyzed morphologically and by flow cytometry using a FACSCalibur flow cytometer (BD Biosciences).

Acquisition of microscopic images

Microscopic images were obtained and analyzed by an Olympus BX53 microscope (Olympus, Tokyo, Japan) equipped with a 100 ×/1.40 numeric aperture oil objective. Images were acquired with a DP73 CCD camera (Olympus) using cellSens software (Olympus) and were processed using Adobe Photoshop version 21.0.1.

Flow cytometry

Immunophenotypic analysis was performed by flow cytometric analysis using fluorochrome- or biotin-conjugated monoclonal antibodies described above and a FACSAria flow cytometer (BD Biosciences).

Chromatin immunoprecipitation (ChIP) and ChIP-Seq

A total of 5×10^7 cells per immunoprecipitation were cross-linked with 1% formaldehyde for ten minutes at room temperature. Chromatin was sheared in lysis buffer containing 1% TritonX-100, 0.1% sodium deoxycholate and 0.1% SDS to an average size of 300 - 500 bp through sonication on ice in a Covaris S220 (Covaris) for 20 minutes (30 seconds on, 30 seconds off; high power load). Chromatin immunoprecipitation was then performed with anti-FLAG (Sigma, F7425), anti-C/EBP α (Santa Cruz Biotechnology, sc-61) or anti-histone H3K27Ac (Active Motif, 39133) antibodies pre-conjugated to Protein G magnetic beads. Immunoprecipitated DNA was purified and subjected to next generation sequencing. Libraries were prepared according to instructions accompanying Illumina's DNA Sample Kit (Part# 0801-0303). Briefly, DNA was end-repaired using a combination of T4 DNA polymerase, *E. coli* DNA Pol I large fragment (Klenow polymerase) and T4 polynucleotide kinase. The blunt, phosphorylated ends were treated with Klenow fragment (32 to 52 exo minus) and dATP to yield a protruding 3- 'A' base for ligation of Illumina's adapters that have a single 'T' base overhang at the 3' end. After adapter ligation, DNA was PCR amplified with Illumina primers for 15 cycles and library fragments of ~250 bp (insert plus adaptor and PCR primer sequences) were band isolated from an agarose gel. The purified DNA was captured on an Illumina flow cell for cluster generation. Libraries were sequenced on the Genome Analyzer following the manufacturer's protocols. Base calls were performed using Bowtie 1.1.1. ChIP-seq reads were aligned to the mm9 genome assembly using samtools 1.2. Peaks were called using

MACS1.4 with the following setting: ChIP threshold (0.2), Enrichment Fold (2.5), Rescue Fold (3). The enriched genomic regions were determined using CisGenome. Overlapping of Trib1, C/EBP α or H3K27Ac peaks was determined using an intersect function of BEDtools. The results were visualized using IGV_2.3.80 (<http://software.broadinstitute.org/software/igv>). Hoxa9 and C/EBP α binding motifs were searched using the AME (MEME-Suit version 4.11.2) program (<http://meme-suite.org/index.html>). Super-enhancers were identified using the method previously described with the ROSE program (http://younglab.wi.mit.edu/super_enhancer_code.html). Gene ontology analysis for super-enhancers were performed by GREAT version 4.0.4 (<http://great.stanford.edu/public/html/>).

Microarray analysis

GeneChip analysis was conducted to determine gene expression profiles. Total RNA was extracted using the RNeasy Mini Kit (QIAGEN). The murine Genome 430 PM Array (Affymetrix) was hybridized with aRNA probes generated from H9M1 cells. After staining with streptavidin-phycoerythrin conjugates, arrays were scanned using an Affymetrix GeneAtlas Scanner and analyzed using Affymetrix GeneChip Command Console Software (AGCC, Affymetrix) and GeneSpring GX 11.0.2 (Agilent Technologies). Gene Set Enrichment Analysis (GSEA) was performed using GSEA-P 2.0 software.

Immunoblotting

Western blot analysis was performed using whole cell lysates with specific antibodies listed in supplemental Table 2.

RT-PCR and real-time quantitative RT-PCR

Total RNA extraction, reverse transcription and RNA quantification were performed by standard methods. Conventional RT-PCR and real-time quantitative RT-PCR (Q-RT-PCR) were performed with a Gene Amp 9700 thermal cycler (Applied Biosystems) and a 7500 Fast Real-Time PCR System (Applied Biosystems), respectively. The sequences of the oligonucleotide primers are shown in Supplemental Table 2.

RNA interference studies and CRISPR/Cas9-mediated gene editing

For knockdown of mouse *Trib1*, *Erg* and *Cebpa*, and human *TRIB1* lentivirus plasmids containing shRNAs were purchased from Sigma. A lentivirus plasmid containing short guided RNA (sgRNA) for *Erg* was purchased from Addgene. The shRNA and sgRNA sequences are listed in supplemental Table S1. Knockdown efficiencies were confirmed by Western blotting or RT-PCR.

***In vivo* drug treatment**

JQ-1 and THZ1 were purchased from Selleck Chemicals (Houston TX), while cytarabine and daunorubicin were purchased from Wako Pure Chemicals (Osaka, Japan). JQ-1 (50 mg/kg) was intraperitoneally administered to mice five times per week for 3 weeks after one week after bone marrow transplantation of *Trib1* hi cells. Cytarabine (100 mg/kg) was given intraperitoneally three times and daunorubicin (1 mg/kg) was injected into the tail vein once. Mice were monitored carefully by checking white blood cell counts, Giemsa staining and GFP-positive fractions in peripheral blood.

Statistics

All *in vitro* experiments were performed at least in triplicate. The numbers of mice used in each experiment are presented in the text or figure legends. Values are expressed as mean \pm SD, and statistical significances were compared with 2-tailed Student's *t* test. Survival analysis was performed using the Kaplan-Meier life table method, and survival between groups was compared with the log-rank test. All *P* values were 2 sided, and a *P* value of less than 0.05 was considered significant.

Supplemental Table 1. The list of shRNA and sgRNA sequences

shRNA	Target sequence	Species
Erg_1	AGCGCTACGCCTACAAGTTTG	Mouse
Erg_2	CCCGAAGCTACGCAAAGAATT	Mouse
Cebpa_1	TGCGAGCACGAGACGTCTATA	Mouse
Cebpa_2	AGCCGAGATAAAGCCAAACAA	Mouse
TRIB1_1	GACTCAGAAATAGGAACTTCA	Human
TRIB1_2	AGCTTAGGAAGTTCGTCTTCT	Human
non-target	CAACAAGATGAAGAGCACCAA	Mammalian
sgRNA	Target sequence	Species
Erg	AGAATGTCGGCATTGTAGCT	Mouse
+85 enhancer	CATTATGGCCAGCACTATTA	Mouse
non-target	AACCGTACTGCGAGGAGCAT	Mammalian

Table S2. List of antibodies

Antibody	Species	Company (Catalog#)	Use*
FLAG M2	Mouse	Sigma (F3165)	WB
FLAG	Rabbit	Sigma (F7425)	ChIP
C/EBP α	Rabbit	Cell Signaling (#2295)	WB
C/EBP α	Rabbit	SantaCruz (sc-61)	ChIP
Mac1 APC	Mouse	eBioScience (17-0112-83)	FACS
Gr-1 PerCP-Cy5.5	Rat	Invitrogen (45-5931-80)	FACS
CD34 PerCP-Cy5.5	Mouse	BioLegend (128607)	FACS
F4/80 APC	Mouse	Invitrogen (17-4801-82)	FACS
Phospho-Erk1/2	Rabbit	Cell Signaling (#9101)	WB
Erk1/2	Rabbit	Cell Signaling (#9102)	WB
Histon H3K27ac	Rabbit	Active motif (#39133)	ChIP
ERG	Rabbit	abcam (ab92513)	WB
c-Myc	Mouse	Santa Cruz (sc-40)	WB
CRISPR-Cas9	Mouse	Novus (NBP2-36440)	WB
GAPDH	Mouse	HyTest (5G4)	WB
α -Tubulin	Mouse	Sigma (T5168)	WB

*Antibodies were used for Western blotting, Chromatin immunoprecipitation (ChIP) and FACS.

Table S3. List of primers

RT-PCR	Forward	Reverse	Species
Erg	TGAGCGCAGAGTGATCGTCC	GCACAGCTCCTTCCCATCGA	Mouse
Spns2	TGGTCTGCTGTACCTTCTCG	CGCCAATGATGGTGGGTGCT	Mouse
Rgl1	GCGGCCAATAAAGGAGCGAG	CCAAAAGCCGTCAGCAGGTT	Mouse
Hspa4	TGCGAATGCTTCAGACCTCC	GGCGGCTCCACTCTTGCTAG	Mouse
Pik3cd	GTCTGCCTGAGCTTAGCTGC	GCGCCAGCCAGTTGACTTTG	Mouse
Tbc1d9b	CGACAACGAGGAGGACATCAC	CCGAACTGCTTCCGCATCTT	Mouse
Lfng	GCCGTCAAGACCACCAGAAAG	TGAGCTTGCCAGAGCTTCG	Mouse
Atg7	GGGACCTGTGAGCTTGGATC	GAAGTAGGGCAGGGCCGTGA	Mouse
Il6ra	CATGTCCCTGCCACATTCC	GTGGGCCCAAGGAATACGGT	Mouse
FLAG-Hoxa9	TACAAGGATGACGATGACAAG	GGGTGGTGGTGGTGTGATGATA	Mouse
FLAG-Trib1	TACAAGGATGACGATGACAAG	GCAGCTGGATGTAAGGCCTG	Mouse
FLAG-Trib2	TACAAGGATGACGATGACAAG	CCAGAGGCTCCAACAGTAAGT	Mouse
Gapdh	TCCGTCGTGGATCTGACGTG	CCGGCATCGAAGGTGGAAGA	Mouse
Actb	AGGCTCTTTCCAGCCTTCC	ATCCTGTCAGCAATGCCTGG	Mouse
TRIB1	GTTCGTCTTCTCCACGGAGG	CGGAGTAGGTCCCAGTGGTG	Human
HOXA9	CTGAGAATGAGAGCGGCGGA	CCAGTTCAGGGTCTGGTGT	Human
ERG	CAGCCAGGGTCACCATCAAA	GGTGGCATGTGCTTCTCCTC	Human
SPNS2	CACCTTCTCCAGCTCCTTCATT	CCCAGTGGGATGGCGAAGTA	Human
RGL1	GCTTGTGGAGAACCTGCTGAC	CACAGTTTGGGCTTGTCAGGT	Human
PIK3CD	GTCATCCAGGGCAGCAAAG	GATGTCGAACTCCAGCCGCT	Human
ACTB	AGAGCTACGAGCTGCCTGAC	AGCACTGTGTTGGCGTACAG	Human
ChIP-PCR	Forward	Reverse	Species
Erg_1	CGGATGCCGGAAGGTAGACG	TTCCTAAGGAGGCCACAGC	Mouse
	chr16:95677674-95677817		
Erg_2	AAGTCCTCACGGCCATCTTCC	GGCGTTTCATTTCGGGAGAGG	Mouse
	chr16:95678509-95678665		
Erg_3	ACTGCATGGACCTCTGAAACAC	GCACAGAGATGGCAAGTGAC	Mouse
	chr16:95679684-95679847		
Spns2_1	TAGGGAGAGCCAGAGACACC	GCCTCCAGAGTGCTGGGATT	Mouse
	chr11:72297651-72297805		
Spns2_2	ACCCAATCAGCAAGCTCCAG	GTATGTGGGCACGTGTGAGC	Mouse

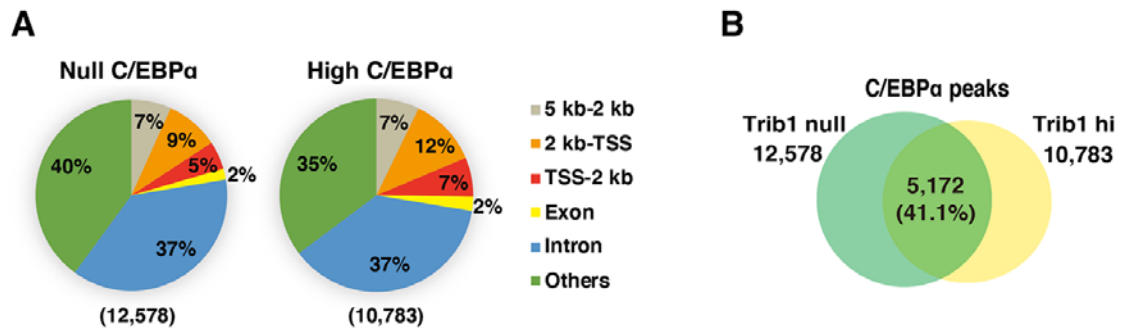
	chr11:72300277-72300435		
Spns2_3	TGGCAAAGCCAGTAAGTAGCAG	CTCACCCCTTCCTCAGATCC	Mouse
	chr11:72297993-72298171		
Rgl1_1	TCCTGCGACAGGCTGCTAAG	CATGACAGCCAGGACTGCAC	Mouse
	chr1:154463289-154463443		
Rgl1_2	TGTGCCACAGCAAACACACC	TTGGCAGGCAGAGGTCTTGG	Mouse
	chr1:154464058-154464231		
Rgl1_3	CACCCACCCACCAAGTTCTG	CAAGCTGCACTGTGGAGAGG	Mouse
	chr1:154464574-154464758		
Pik3cd_1	GATCTGGGCCACAGGAGGAC	GGCCACAGTGCGGTCTTTTG	Mouse
	chr4:149037480-149037635		
Pik3cd_2	AACCAGCTTGATGACCGTGAG	TGAGGGTTGGCATGACCGAT	Mouse
	chr4:149037862-149038015		
Pik3cd_3	AGGCTTGTGCAGGTAGGTCC	CCCTCCTCCAAGTCTGTGCA	Mouse
	chr4:149038312-149038500		
Chek1	ACCCGCTCACTTCCAATTCC	CCCGTGGCTCTCCAGCATAA	Mouse
Erg +85	TGGGCAGCCAGGACCAATAG	CTAGGCAGCGCAAAGGAAATCT	Mouse

Supplemental Table 5. The list of human AML cell lines.

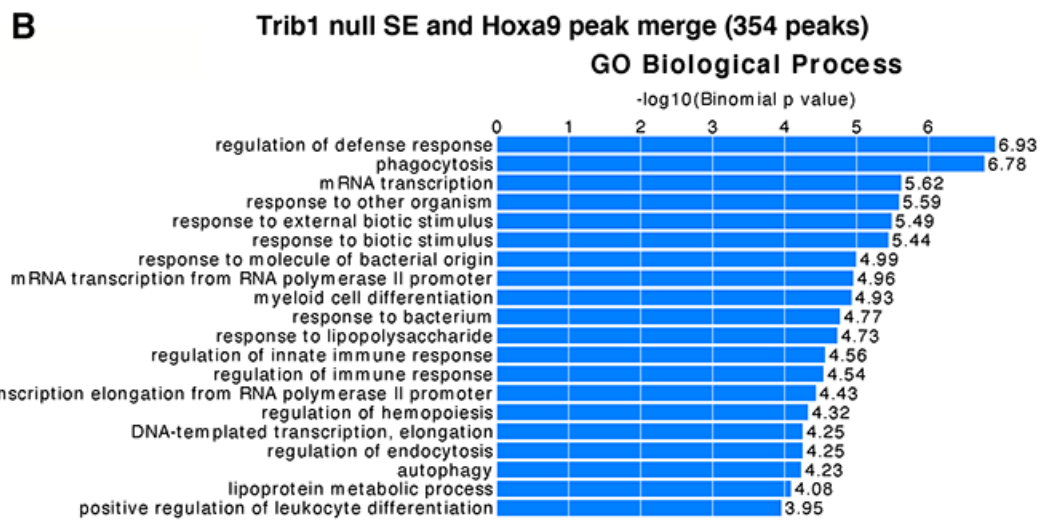
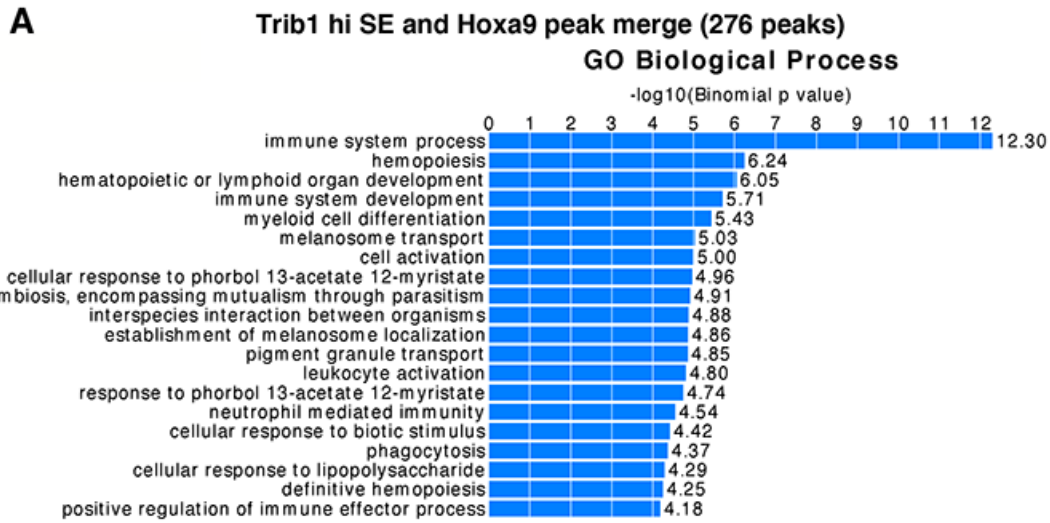
Cell line	Lineage	Genetic lesion
HEL	AML, M6	t(1;6)(p13;p21), t(3;6)(p13;q16), t(5;17)(q11;p11), del20(q12)
HL-60	AML, M3	9p-, t(10;13), NRAS (Q61L)
KU812	CML-BC*	BCR-ABL1
P39	AML-MDS**	del6(q15), 9q+, t(14;16)(q24;q21), -16, -17
THP1	AML, M5	MLL-AF9, NRAS (G12D)

*CML-BC: Blastic crisis of chronic myelogenous leukemia.

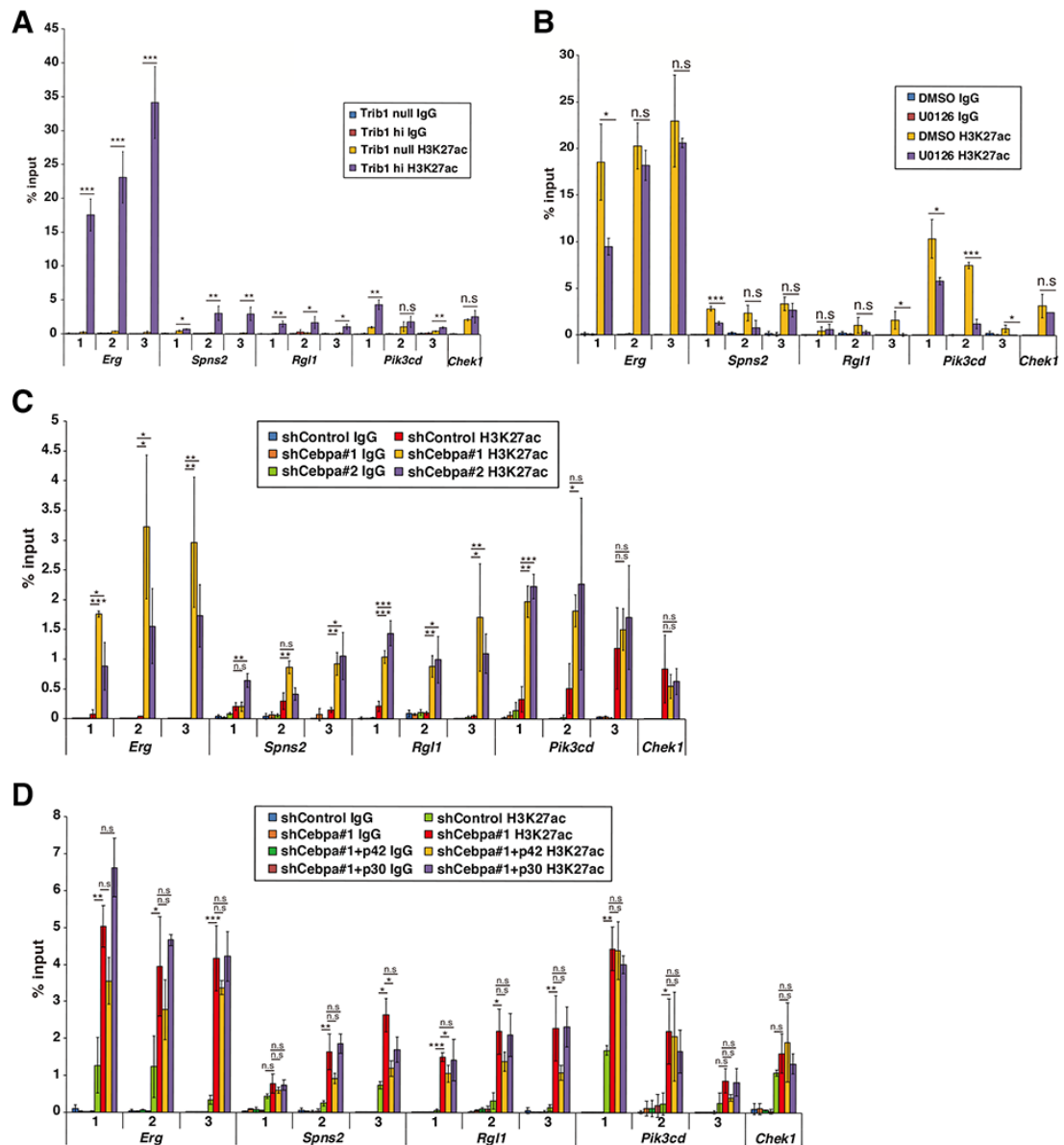
**AML-MDS: overt AML derived from myelodysplastic syndrome



Supplemental Figure 1. C/EBP α binding peaks in Trib1 null and high cells. (A) Global distribution of Hoxa9 binding peaks. (B) Venn diagram showing frequent overlaps of C/EBP α binding peaks between Trib1 null and high cells.

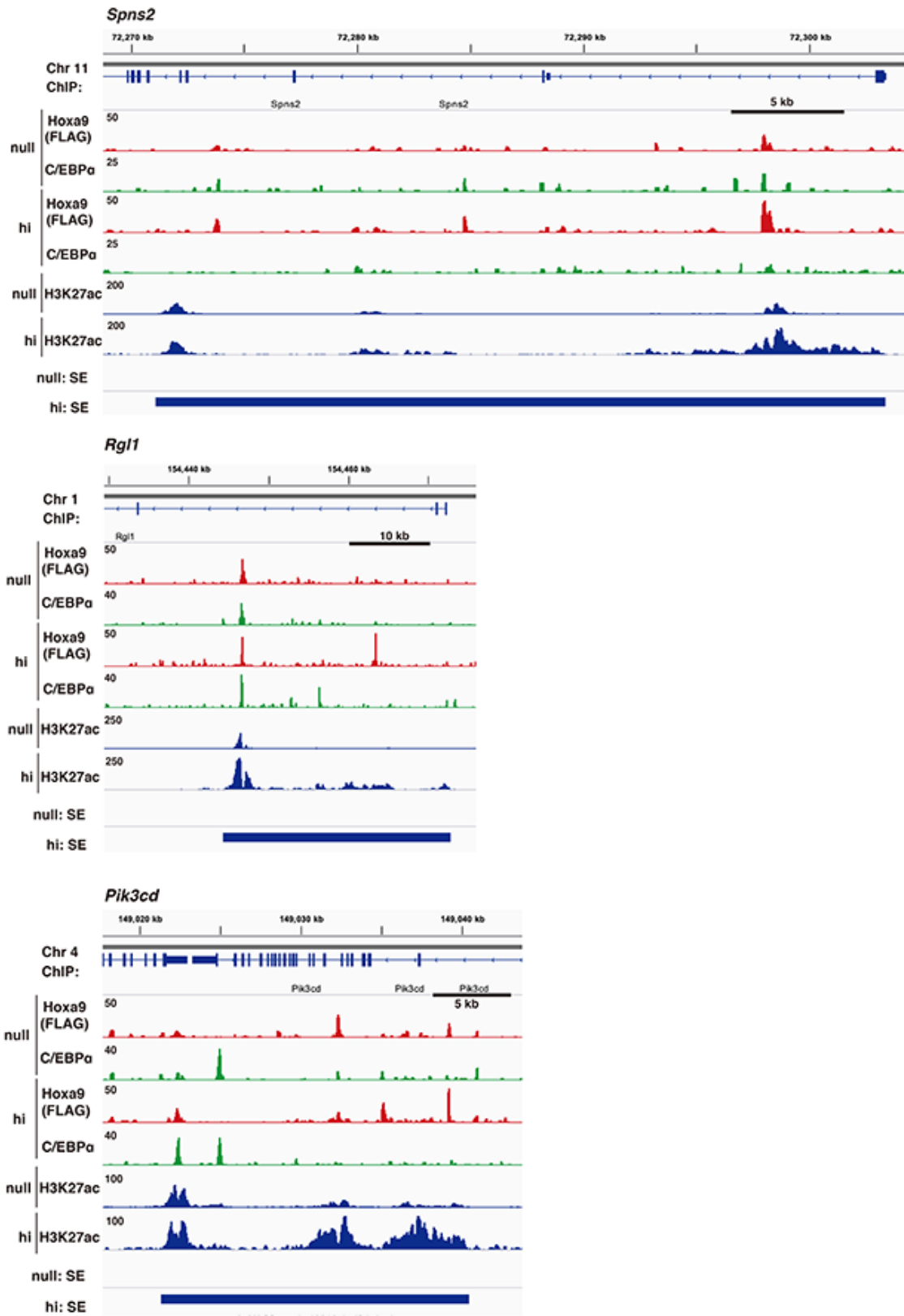


Supplemental Figure 2. Enrichment of gene ontology biological process for Trib1 hi (A) and Trib1 null (B) super-enhancer loci.



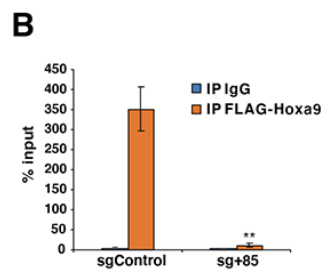
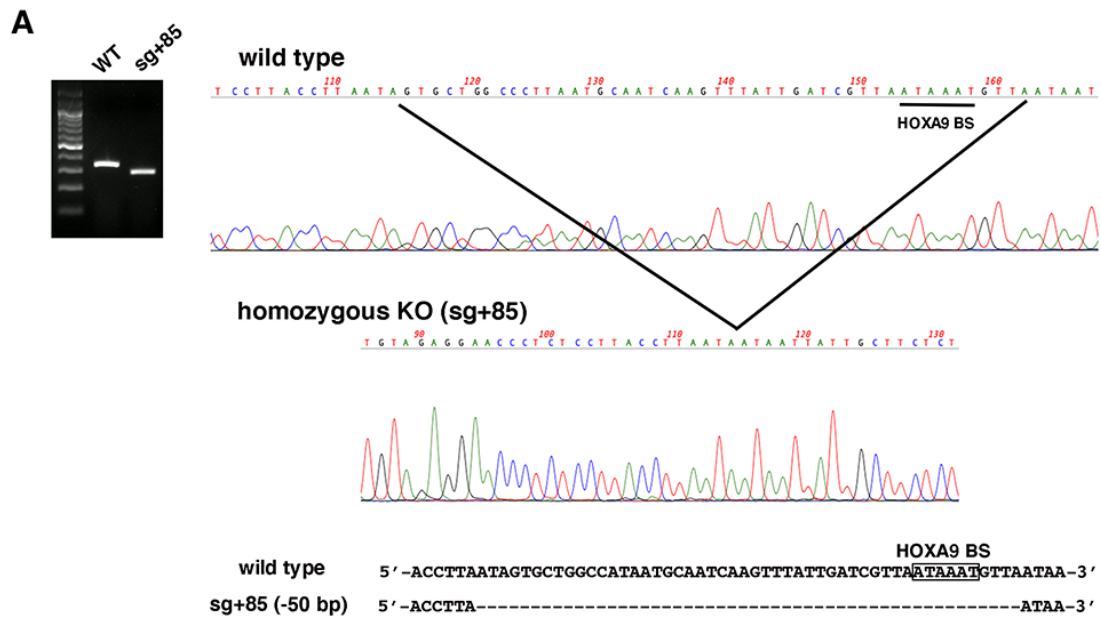
Supplemental Figure 3. Quantitative ChIP-PCR for super-enhancers. The results are shown as three different loci in each super-enhancer. (A) Quantitative ChIP-PCR of H3K27ac relative signals for super-enhancers of *Erg*, *Spns2*, *Rgl1*, and *Pik3cd*. The *Chek1* locus is shown as a negative control. Average accumulation quantities in three loci are shown in Figure 3E. (B) Quantitative ChIP-PCR of H3K27ac upon U0126 treatment. Average accumulation quantities in three loci are shown in Figure 4A. (C) Quantitative ChIP-PCR of H3K27ac upon *Cebpa* silencing. Average accumulation quantities in three loci are shown in Figure 4C. (D) Quantitative ChIP-PCR of H3K27ac upon *Cebpa*

silencing with or without p42 or p30. Average accumulation quantities in three loci are shown in Figure 4E.

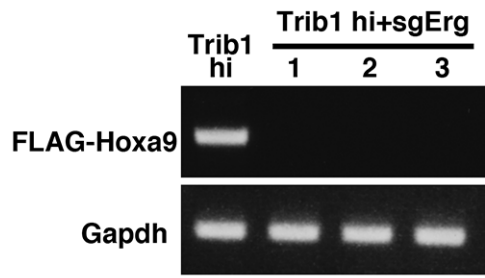


Supplemental Figure 4. Super-enhancers modulated by Trib1. Density plots for ChIP-

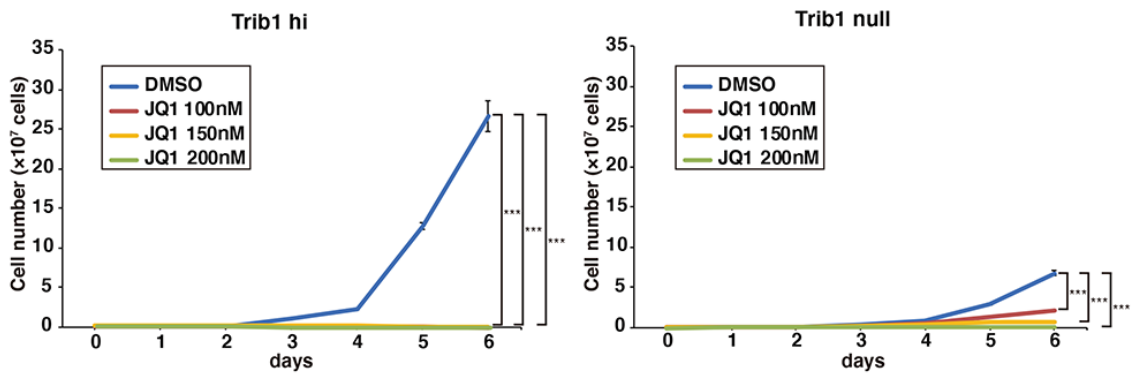
seq reads for C/EBP α , Hoxa9 and H3K27ac in Trib1 hi and null cells at the super-enhancers of *Spns2*, *Rgl1* and *Pik3cd* loci.



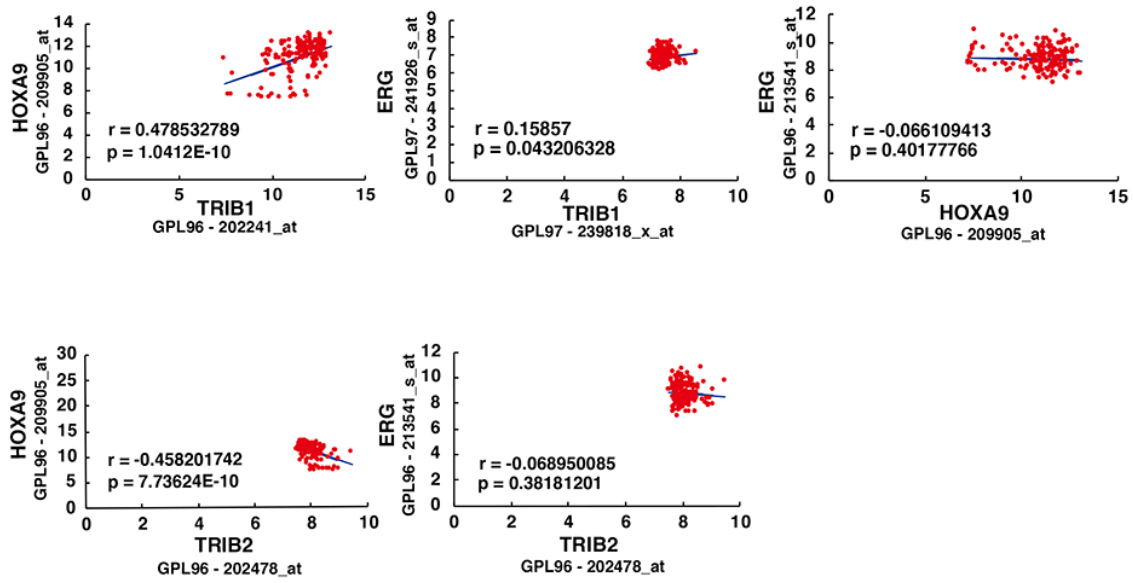
Supplemental Figure 5. CRISPR/Cas9-mediated deletion of the *Erg* +85 enhancer sequence. (A) Genomic PCR (left) and direct sequencing (right) show homozygous deletion of 50 bp containing Hoxa9 binding sequence (HOXA9 BS) within the +85 enhancer. (B) Quantitative ChIP-PCR showing relative signals of FLAG-Hoxa9 to input DNA (bottom). * $P < 0.05$, ** $P < 0.01$.



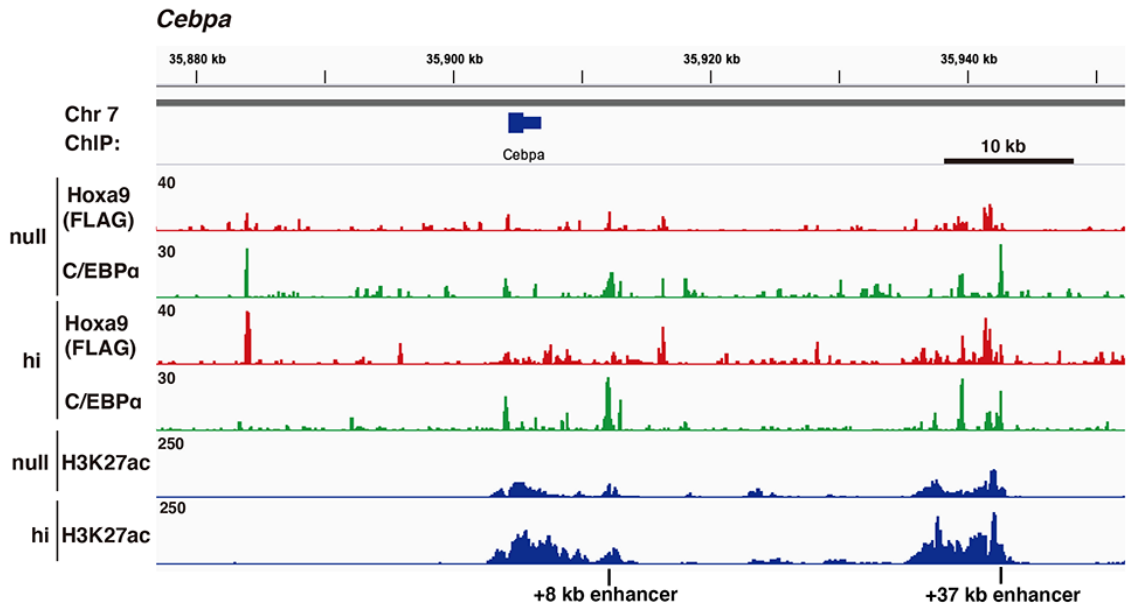
Supplemental Figure 6. Absence of the *Hoxa9*-positive leukemic cell fraction in the recipients transplanted with *Erg*-silenced Trib1 hi cells. RT-PCR showed of bone marrow cells showed no FLAG-*Hoxa9* expression in three recipients.



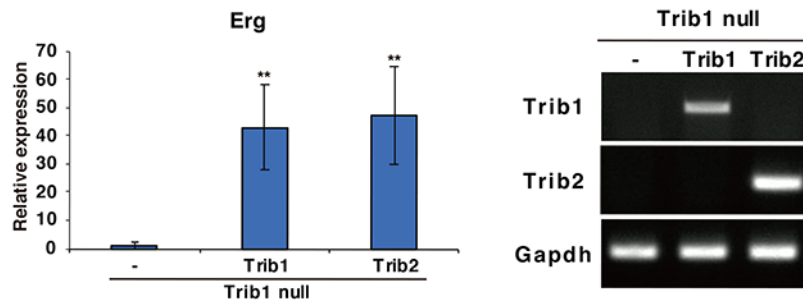
Supplemental Figure 7. Growth of Trib1 hi (left) and null (right) cells treated with JQ1 or vehicle for longer duration than those shown in Figure 6A.



Supplemental Figure 8. Correlative gene expression for *HOXA9*, *ERG*, *TRIB1* and *TRIB2* in the human cohort. Pearson's correlation test was performed using the human AML cohort used in Figure 7F (GSE12417 of GEO).



Supplemental Figure 9. Density plots for ChIP-seq reads for C/EBP α , Hoxa9 and H3K27ac in Trib1 hi and null cells at the *Cebpa* locus.



Supplemental Figure 10. Upregulation of *Erg* by *Trib1* or *Trib2* overexpression in *Trib1* null cells. Quantitative RT-PCR shows increased expression of *Erg* (left). Expression of *Trib1* and *Trib2* in *Trib1* null cells is confirmed by RT-PCR (right).